

**Note to readers with disabilities:** *EHP* strives to ensure that all journal content is accessible to all readers. However, some figures and Supplemental Material published in *EHP* articles may not conform to [508 standards](#) due to the complexity of the information being presented. If you need assistance accessing journal content, please contact [ehp508@niehs.nih.gov](mailto:ehp508@niehs.nih.gov). Our staff will work with you to assess and meet your accessibility needs within 3 working days.

### **Supplemental Material**

#### **Association between Organophosphate Ester Exposure and Insulin Resistance with Glycometabolic Disorders among Older Chinese Adults 60–69 Years of Age: Evidence from the China BAPE Study**

Enmin Ding, Fuchang Deng, Jianlong Fang, Tiantian Li, Minmin Hou, Juan Liu, Ke Miao, Wenyan Yan, Ke Fang, Wanying Shi, Yuanzheng Fu, Yuanyuan Liu, Haoran Dong, Li Dong, Changming Ding, Xiaohui Liu, Krystal J. Godri Pollitt, John S. Ji, Yali Shi, Yaqi Cai, Song Tang, and Xiaoming Shi

#### **Table of Contents**

**Table S1.** Variable information of 17 blood OPEs and 11 urine OPE metabolites.

**Table S2.** Descriptive statistics of the results from the daily time-activity surveys (for the three consecutive days prior to the physical examination) of participants for each of the five visits.

**Table S3.** Changes in the z-scores of glycometabolic markers with a quantile increase in the mixture concentration.

**Table S4.** Relative weight of each pollutant within four chemical mixtures.

**Table S5.** Proportions and overall averages of associated serum metabolite in each class for the key OPEs.

**Table S6.** Proportions and overall averages of the associated urine metabolite in each class for the key OPEs.

**Table S7.** Representative toxicological literature on the associations between OPEs and glycometabolic marker.

**Table S8.** Representative toxicological literature on the molecular mechanisms of OPEs.

**Figure S1.** Pairwise spearman correlations of the 28 OPE exposures.

**Figure S2.** Sensitivity analysis results of the associations between OPE exposures and glycometabolic markers.

**Figure S3.** Stratification analysis results of the associations between OPE exposures and glycometabolic markers by sex.

**Figure S4.** Common and specific biomolecular intermediators of individual OPEs.

## **References**

**Additional File-** Excel Document

## Supplemental Tables

**Table S1.** Variable information of 17 blood OPEs and 11 urine OPE metabolites.

No.	Family	Abbreviation	Full name	Detection frequency (%)	LOD	Median (P25-P75)	IQR	SD	ICC	Transformation
1	Blood	TPHP	Tri-phenyl phosphate	78	0.11	0.40 (0.14-1.70)	1.56	1.24	0.16	Log10
2	OPEs	EHDPP	2-Ethylhexyl di-phenyl phosphate	77	0.03	0.21 (0.04-0.40)	0.35	0.30	0.04	Power 1/3
3		TCIPP	Tri(1-chloro-2-propyl) phosphate	77	0.13	0.74 (0.19-1.36)	1.17	0.92	0.05	Power 1/3
4		TnBP	Tri-n-butyl phosphate	59	0.15	0.25 (0.07-0.62)	0.54	0.75	0.05	Log10
5		TCEP	Tri(2-chloroethyl) phosphate	56	0.22	0.30 (0.11-0.77)	0.66	0.56	0.03	Log10
6		TBP	Tributyl phosphate	55	0.20	0.49 (0.10-1.31)	1.21	1.51	0.04	Log10
7		TEP	Triethyl phosphate	54	0.06	0.14 (0.03-0.72)	0.69	1.29	0.04	Log10
8		TiBP	Tri-iso-butyl phosphate	51	0.22	0.23 (0.11-0.75)	0.64	0.89	0.03	Log10
9		TEHP	Tris(2-ethylhexyl) phosphate	51	0.09	0.09 (0.04-0.38)	0.34	0.50	0.06	Log10
10		BABP	Bisphenol-A bis(diphenyl phosphate)	47	0.004	0.002 (0.002-0.01)	0.01	0.01	0.02	Log10
11		TBOEP	Tri(2-butoxyethyl) phosphate	41	0.05	0.03 (0.03-0.20)	0.18	0.70	0.03	Log10
12		TDCPP	Tris(1,3-dichloro-2-propyl) phosphate	34	0.21	0.11 (0.11-0.32)	0.21	0.32	0.02	Log10
13		TMPP	Trimethylphenyl phosphate	33	0.02	0.01 (0.01-0.04)	0.03	0.03	0.04	Log10
14		RDP	Resorcinol bis(diphenyl phosphate)	21	0.02	0.01 (0.01-0.01)	0.00	0.06	0.02	Log10
15		TMP	Trimethyl phosphate	16	0.15	0.07 (0.07-0.07)	0.00	0.67	0.01	Log10
16		CDPP	Cresyl diphenyl phosphate	7	0.17	0.08 (0.08-0.08)	0.00	0.13	0.02	Log10
17		TPrP	Tripropyl phosphate	1	0.02	0.01 (0.01-0.01)	0.00	0.01	0.001	Log10
18	Urine	DPHP	Di-phenyl phosphate	79	0.04	0.11 (0.07-0.19)	0.11	0.46	0.02	Log10
19	OPE	DEHP	Di(2-ethylhexyl) phosphate	77	0.07	0.21 (0.09-0.41)	0.32	1.61	0.02	Log10
20	metabolite	BDCPP	Bis(1,3-dichloro-2-propyl) phosphate	76	0.05	0.16 (0.07-0.28)	0.20	0.31	0.02	Log10
21		DBP	Dibutyl phosphate	69	0.01	0.07 (0.03-0.18)	0.15	0.15	0.09	Log10
22		BMPP	Bis(2-methylphenyl phosphate)	65	0.004	0.02 (0.01-0.03)	0.02	0.03	0.18	Log10
23		BCIPP	Bis(1-chloro-2-propyl) phosphate	28	0.04	0.04 (0.03-0.08)	0.05	0.14	0.06	Log10

24	DPHP-OH	Hydroxyphenyl diphenyl phosphate	21	0.02	0.02 (0.01-0.04)	0.03	0.06	0.05	Log10
25	BCEP	Bis(2-chloroethyl) phosphate	20	0.63	0.52 (0.35-1.03)	0.69	2.08	0.11	Log10
26	BBOEP	Bis(2-butoxyethyl) phosphate	13	0.03	0.02 (0.02-0.05)	0.03	1.58	0.002	Log10
27	EHDPP-OH	Hydroxyphenyl 2-ethylhexyl-diphenyl phosphate	13	0.04	0.003 (0.002-0.01)	0.00	0.05	0.01	Log10
28	BBOEHEP	Bis(2-butoxyethyl) hydroxyethyl phosphate	3	0.02	0.02 (0.01-0.03)	0.01	0.06	0.06	Log10

---

Note: unit for LOD is  $\mu\text{g/L}$ ; unit for blood OPEs is  $\mu\text{g/L}$ , and unit for urine OPE metabolites is  $\mu\text{g/g}$  creatinine; LOD: limit of detection; IQR: inter-quartile range; SD: standard deviation; ICC: intra-class correlation coefficient.

**Table S2.** Descriptive statistics of the results from the daily time-activity surveys (for the three consecutive days prior to the physical examination) of participants for each of the five visits.

Characteristics	1 <sup>st</sup> (N=66)	2 <sup>nd</sup> (N=74)	3 <sup>rd</sup> (N=71)	4 <sup>th</sup> (N=71)	5 <sup>th</sup> (N=71)
Extra Diet in last 72h	Number of subjects (% subject population)				
Fruit	27 (40.9)	38 (51.4)	35 (49.3)	34 (47.9)	39 (54.9)
Milk	3 (4.5)	4 (5.4)	5 (7.0)	4 (5.6)	4 (5.6)
Rice	5 (7.6)	13 (17.6)	7 (9.9)	11 (15.5)	10 (14.1)
Nuts	4 (6.1)	10 (13.5)	16 (22.5)	21 (29.6)	18 (25.4)
Eggs	0 (0)	0 (0)	0 (0)	2 (2.8)	1 (1.4)
Seafood	2 (3.0)	5 (6.8)	3 (4.2)	2 (2.8)	1 (1.4)
Meat	3 (4.5)	2 (2.7)	3 (4.2)	2 (2.8)	3 (4.2)
Vegetables	2 (3.0)	4 (5.4)	7 (9.9)	10 (14.1)	5 (7.0)
Bean products	0 (0)	2 (2.7)	0 (0)	1 (1.4)	1 (1.4)

**Table S3.** Changes in the z-scores of glycometabolic markers with a quantile increase in the mixture concentration.

Glycometabolic markers	Quantile midpoint	Line predication	Low limit of line predication	Up limit of linpred	Low limit of simulation	Up limit of simulation
FPG	0.13	0.77	0.72	0.82	0.74	0.79
FPG	0.38	0.82	0.79	0.84	0.79	0.84
FPG	0.63	0.86	0.86	0.86	0.81	0.91
FPG	0.88	0.91	0.89	0.94	0.84	0.98
GSP	0.13	2.49	2.44	2.54	2.47	2.51
GSP	0.38	2.53	2.51	2.55	2.50	2.55
GSP	0.63	2.57	2.57	2.57	2.52	2.61
GSP	0.88	2.61	2.58	2.63	2.53	2.68
FINS	0.13	0.44	0.37	0.51	0.36	0.51
FINS	0.38	0.49	0.46	0.53	0.46	0.53
FINS	0.63	0.55	0.55	0.55	0.51	0.59
FINS	0.88	0.61	0.57	0.64	0.54	0.68
HOMA-IR	0.13	-0.13	-0.30	0.04	-0.24	-0.01
HOMA-IR	0.38	-0.01	-0.09	0.07	-0.09	0.07
HOMA-IR	0.63	0.11	0.11	0.11	-0.04	0.25
HOMA-IR	0.88	0.23	0.14	0.31	-0.01	0.44

Note: see also **Figure 3B**.

**Table S4.** Relative weight of each pollutant within four chemical mixtures.

Pollutant	FPG		Pollutant	GSP		Pollutant	FINS		Pollutant	HOMA-IR	
	Negative weight	Positive weight		Negative weight	Positive weight		Negative weight	Positive weight		Negative weight	Positive weight
TPHP	-	0.14	TPHP	-	0.19	TPHP	-	0.44	TPHP	-	0.17
TMPP	-	0.54	TMPP	-	0.46	DPHP	-	0.13	TnBP	-	0.06
EHDPP	1.00	-	EHDPP-OH	0.03	-	DBP	-	0.43	TMPP	-	0.20
DPHP	-	0.01	EHDPP	0.97	-				TiBP	-	0.29
DBP	-	0.24	DPHP	-	0.02				TBP	0.24	-
BCEP	-	0.07	DBP	-	0.26				EHDPP	0.57	-
			BCEP	-	0.07				DPHP	-	0.06
									DBP	-	0.23
									BCEP	0.18	-

Note: see also **Figure 3C**.

**Table S5.** Proportions and overall averages of associated serum metabolite in each class for the key OPEs.

Pollutant	Serum Metabolite								
	Amino Acid	Carbohydrate	Cofactors and Vitamins	Energy	Lipid	Nucleotide	Partially Characterized Molecules	Peptide	Xenobiotics
TMPP	12.38% 4.76%	0.00% 22.73%	21.05% 2.63%	20.00% 10.00%	3.96% 18.18%	20.51% 20.51%	8.33% 0.00%	43.18% 31.82%	6.54% 3.27%
TPHP	13.33% 14.29%	4.55% 36.36%	23.68% 15.79%	30.00% 20.00%	7.93% 26.34%	20.51% 23.08%	33.33% 8.33%	47.73% 29.55%	4.58% 7.19%
TiBP	1.43% 3.33%	9.09% 9.09%	5.26% 0.00%	10.00% 0.00%	0.70% 2.80%	0.00% 5.13%	0.00% 0.00%	9.09% 22.73%	1.31% 3.92%
DBP	2.38% 6.19%	0.00% 9.09%	5.26% 13.16%	0.00% 20.00%	2.56% 5.59%	0.00% 7.69%	8.33% 8.33%	2.27% 4.55%	11.76% 7.19%
DPHP	0.95% 1.43%	0.00% 0.00%	5.26% 5.26%	0.00% 0.00%	3.03% 0.93%	0.00% 5.13%	0.00% 0.00%	0.00% 2.27%	1.96% 0.00%
Total	30.47% 30.00%	13.64% 77.27%	60.51% 36.84%	60.00% 50.00%	18.18% 53.84%	40.12% 61.54%	49.33% 16.66%	102.25% 90.92%	26.15% 21.57%
Average	6.10% 6.00%	2.73% 15.45%	12.11% 7.37%	12.00% 10.00%	3.64% 10.77%	8.21% 12.31%	10.00% 3.33%	20.45% 18.18%	5.23% 4.31%

Note: red (left) and blue (right) colors represent positive and negative associations, respectively; see also **Figure 4F**.



**Table S6.** Proportions and overall averages of the associated urine metabolite in each class for the key OPEs.

Pollutant	Urine Metabolite								
	Amino Acid	Carbohydrate	Cofactors and Vitamins	Energy	Global	Lipid	Nucleotide	Other	Other secondary metabolites
TMPP	0.00% 0.42%	0.00% 0.00%	0.00% 0.00%	0.00% 0.00%	0.00% 0.00%	0.00% 0.00%	0.00% 1.69%	0.00% 0.00%	0.00% 0.00%
TPHP	1.26% 3.77%	5.48% 5.48%	7.50% 2.50%	0.00% 20.00%	3.45% 0.00%	0.00% 6.52%	0.00% 11.86%	2.03% 5.41%	0.00% 10.00%
TiBP	0.84% 0.00%	0.00% 0.00%	5.00% 0.00%	0.00% 0.00%	0.00% 0.00%	0.00% 0.00%	0.00% 0.00%	0.00% 0.00%	0.00% 0.00%
DBP	12.97% 21.34%	26.03% 24.66%	15.00% 22.50%	20.00% 0.00%	0.00% 31.03%	6.52% 23.91%	10.17% 42.37%	9.01% 17.79%	40.00% 0.00%
DPHP	10.88% 17.99%	19.18% 17.81%	10.00% 27.50%	0.00% 0.00%	10.34% 27.59%	4.35% 21.74%	6.78% 28.81%	10.14% 12.39%	10.00% 0.00%
Total	25.95% 43.52%	50.69% 47.95%	37.50% 52.50%	20.00% 20.00%	13.79% 58.62%	10.87% 52.17%	16.95% 84.73%	21.18% 35.59%	50.00% 10.00%
Average	5.19% 8.70%	10.14% 9.59%	7.50% 10.50%	4.00% 4.00%	2.76% 11.72%	2.17% 10.43%	3.39% 16.95%	4.23% 7.12%	10.00% 2.00%

Note: red (left) and blue (right) colors represent positive and negative associations, respectively; see also **Figure 4G**.

**Table S7.** Representative toxicological literature on the associations between OPEs and glycometabolic marker.

Pollutant	No	Type	Subject	Outcome	Main Results	Journal	Year
TPHP	1	<i>In vivo</i>	Pubertal mice	Adiponectin; HOMA-IR	We observed that the insulin-sensitizing hormone (adiponectin) was inhibited in female serum while stimulated in males after oral administration of TPhP. Correspondingly, we found a high index of HOMA-IR in females.	J Hazard Mater	2020 <sup>2</sup>
	2	<i>In vivo</i>	Adult male mice	Blood biochemistry; Gene expression; Gut microbiota compositions; Metabolic functions	Results showed that TPHP exposure led to increased body weight, liver weight, fat mass, hepatic steatosis, impaired glucose homeostasis, and insulin resistance, and mRNA levels of genes involved in lipid metabolism, especially lipogenesis and lipid accumulation, were significantly altered by TPHP treatment.	Environ Pollut	2019 <sup>3</sup>
	3	<i>In vivo</i>	Earthworm	Metabolome	Acute TPHP exposure caused significant perturbations of the endogenous metabolome in earthworms, featuring fluctuations in amino acids, glucose, inosine and phospholipids.	Sci Rep	2018 <sup>4</sup>
	4	<i>In vivo</i>	Rats	Type 2 diabetes mellitus	Perinatal TPHP exposure accelerated T2DM onset in males and increased plasma non-esterified- fasting fatty acids.	Reproductive Toxicology	2017 <sup>5</sup>
	5	<i>In vivo</i>	Zebrafish	Hepatic histopathological; metabolomic and transcriptomic responses	These results suggest that triphenyl phosphate exposure markedly disturbs hepatic carbohydrate and lipid metabolism in zebrafish. Moreover, DNA replication, the cell cycle, and non-homologous end-joining and base excision repair were strongly affected, thus indicating that triphenyl phosphate hinders the DNA damage repair system in zebrafish liver cells.	Sci Rep	2016 <sup>6</sup>
	6	<i>In vivo</i>	C57Bl/6 mice	Insulin-like growth factor	A significant decrease in transcript levels of Igf1 and Irs2 was detected in maternal livers, whereas a significant increase in transcript levels of all genes measured was detected in fetal liver. A significant decrease in Igf1 protein levels was detected in maternal liver, however the increase in Igf1 protein levels in fetal livers was not found to be statistically significant.	Birth Defects Res	2018 <sup>7</sup>
	7	<i>In vivo</i>	Adult mice	Metabolomics	Both TPP and DPP had no negative effect on uterine weight, glucose tolerance, and estradiol. 1H-NMR-based metabolomics revealed a sex-specific metabolic disturbance of TPP.	Environ Pollut	2018 <sup>8</sup>
	8	<i>In vivo</i>	Female mice	Expression of genes glucose metabolism and xenobiotic metabolism	In the mediobasal hypothalamus, OPFR increased Pdyn, Tac2, Esr1, and Pparg in PND 14 females. In the liver, OPFR increased Pparg and suppressed Insr, G6pc, and Fasn in PND 14 males and increased Esr1, Foxo1, Dgat2, Fasn, and Cyb2b10 in PND 14 females.	Reprod Toxicol	2020 <sup>9</sup>
	9	<i>In vivo</i>	Wild-type C57Bl/6J dams	Glucose homeostasis; metabolism	OPFR exposure interacted with HFD to increase fasting glucose in females and alter glucose and insulin tolerance in male offspring.	J Appl Toxicol	2021 <sup>10</sup>

	10	<i>In vivo</i>	Adult mice	Metabolism	Despite no marked effect of OPFRs on glucose or insulin tolerance, OPFR treatment altered circulating insulin and leptin in females and ghrelin in males.	J Toxicol Environ Health A	2020 <sup>11</sup>
	11	<i>In vivo</i>	adult wild-type (WT) and ER $\alpha$ KO mice	Glucose and insulin tolerance	FR increased fasting glucose levels in males, and BDE-47 augmented glucose clearance in females. In males, OPFR increased ghrelin but decreased leptin and insulin independent of body weight.	Toxicol Sci	2018 <sup>12</sup>
	12	<i>In vivo</i>	Mice	Glucose and insulin tolerance	Interestingly, female PPAR $\gamma$ KO mice, but not males, experienced many novel OPFR effects not noted in WT mice, including decreased fat mass, altered feeding behavior and efficiency, improved insulin sensitivity, elevated plasma ghrelin and hypothalamic expression of its receptor.	J Toxicol Environ Health A	2022 <sup>13</sup>
	13	<i>In vivo</i>	Adult mice	Food intake patterns, glucose and insulin tolerance	Male ER $\alpha$ KO mice fed LFD experienced decreased feeding efficiency and altered insulin tolerance, whereas their female counterparts displayed less fat mass and circulating ghrelin when exposed to OPFRs.	J Toxicol Environ Health A	2022 <sup>14</sup>
	14	<i>In vitro</i>	3T3-L1 cells	Resistin; leptin	Triphenyl phosphate (TPhP), tricresyl phosphate (TCP), TDCPP, TBP and TBEP enhanced glucose uptake at both basal and insulin-stimulated status.	Environ Pollut	2022 <sup>15</sup>
	15	<i>In vitro</i>	Hep G2 cell	Metabolic disturbances	We found that when HepG2 cells were exposed to TMPP, TPHP and TDBPP, the main metabolic sub-network disturbances focused on metabolism linked with oxidative stress, osmotic pressure equilibrium, and glucocorticoid and mineralocorticoid receptor antagonist activities.	Sci Total Environ	2019 <sup>16</sup>
	16	<i>In vitro</i>	3T3-L1 cells	Glucose uptake	This study suggests that TPhP increases adipogenic differentiation, glucose uptake, and lipolysis in 3T3-L1 cells through endocrine and noradrenergic mechanisms.	Toxicol In Vitro	2017 <sup>17</sup>
	17	<i>In vitro</i>	RAW264.7 murine macrophage cells	Lipidomic analysis; insulin resistance	Correspondingly, exposure to 10 and 20 $\mu$ M TPHP induced endoplasmic reticulum (ER) stress and inflammatory responses, which have been linked to metabolic dysfunction such as insulin resistance and hypertriglyceridemia.	Environ Pollut	2020 <sup>18</sup>
DPHP	18	<i>In vitro</i>	3T3-L1 cells	Insulin-stimulated	DPhP increased the insulin-stimulated 2-NBDG uptake only at 100 $\mu$ M DPhP.	Toxicol In Vitro	2017 <sup>17</sup>

**Table S8.** Representative toxicological literature on the molecular mechanisms of OPEs.

Pollutant	Pathway	No	Type	Subject	Outcome	Main results	Journal	Year
TPhP	Oxidative Stress	1	<i>In vivo</i>	Labeo rohita fingerlings	reactive oxygen species (ROS) production; lipid peroxidation (LPO) rates	The reactive oxygen species (ROS) production and lipid peroxidation (LPO) rates were significantly higher in tissues (brain, liver, and kidney) of TPhP-treated groups. Interestingly, superoxide dismutase (SOD) and catalase (CAT) activities were remarkably decreased in tissues following TPhP exposure.	Chem Res Toxicol	2021 <sup>19</sup>
		2	<i>In vivo</i>	Zebrafish	ROS generation; Lipid peroxidation (LPO); Superoxide dismutase (SOD) activity; Catalase (CAT) activity; Glutathione-S-transferase (GST) activity; Antioxidant activities	The hepatic glucose production (except short-term TPhP treatment up to 48 h), aspartate transaminase, alanine transaminase, lactate dehydrogenase, reactive oxygen species generation, lipid peroxide, and catalase activities were found to be increased in TPhP exposed groups when compared to control groups (normal and solvent control groups). Our study reveals that TPhP can potentially cause antioxidants imbalance, alterations in enzymological and biochemical profiles, and morphological anomalies in hepatic tissues of zebrafish.	Neurotoxicol Teratol	2020 <sup>20</sup>
		3	<i>In vitro</i>	Murine dendritic cells	anti-oxidant enzyme hemeoxygenase-1	Concentrations of TPhP and TDCIPP of 50 $\mu$ M were cytotoxic to BMDCs. At these cytotoxic concentrations, TPhP exposure induced an activated phenotype in steady state DCs, while HDM exposed DCs acquired a tolerogenic phenotype. The cytotoxic concentrations induced the anti-oxidant enzyme hemeoxygenase-1, which is a marker for oxidative stress.	Chemosphere	2017 <sup>21</sup>
		4	<i>In vitro</i>	HepaRG cells	biomarkers of the oxidative stress TP	Potential biomarkers belonging to different TPs were found for APAP and TPhP. For APAP, the biomarkers were related to a decrease in unsaturated phospholipids, and for TPhP to an accumulation of phosphoglycerolipids and increase of palmitoyl lysophosphatidylcholine.	Toxicol In Vitro	2015 <sup>22</sup>
		5	<i>In vitro</i>	Non-small cell lung cancer A549 cell	reactive oxygen species (ROS) production	OPFRs and BFRs could cause the reduction of cell viability of A549 cell in both dose- and time-dependent manner after exposure for 24 and 48 h. Simultaneously, excessive generation of reactive oxygen species (ROS), mitochondrial membrane potential (MMP) dysfunction.	Chemosphere	2019 <sup>23</sup>
		6	<i>In vitro</i>	Hep G2 cell line	metabolic disturbances;	When HepG2 cells were exposed to TMPP, TPhP and TDBPP, the main metabolic sub-network disturbances focused on metabolism linked with oxidative stress, osmotic pressure equilibrium, and glucocorticoid and	Sci Total Environ	2019 <sup>16</sup>

7	<i>In vitro</i>	H4IIE cells	oxidative stress responses (gpx1, gr, gsta2, cat)	mineralocorticoid receptor antagonist activities. Cells treated with TCEP and TPP showed opposite trends between cyp11a1 mRNA and enzymatic activities. Furthermore, exposure to TCEP increased gsta2 and cat especially at the highest concentration tested, whereas TPP produced significant changes only for gr and cat at the highest concentration.	Toxicol Appl Pharmacol	2019 <sup>24</sup>
8	<i>In vitro</i>	TM3 cells	superoxide dismutase (SOD), catalase (CAT), glutathione peroxidase (GPX) and glutathione S-transferase (GST) activities	3 $\beta$ -hydroxysteroid dehydrogenase (3 $\beta$ -HSD) and 17 $\beta$ -hydroxysteroid dehydrogenase (17 $\beta$ -HSD) were dramatically reduced by TPP and TCEP treatments, especially with the high dosage for 24 h. TPP and TCEP treatments for 24 h caused significant decreases in T levels in the medium. Furthermore, co-treatments of hCG with TPP or TCEP could inhibit hCG-induced changes in the expression of P450 <sub>scc</sub> , P450-17 $\alpha$ and 17 $\beta$ -HSD and T levels. TPP and TCEP could induce oxidative stress and endocrine disruption in TM3 cells.	Reprod Toxicol	2015 <sup>25</sup>
9	<i>In vitro</i>	Human normal liver cell (L02)	multi-omic (transcriptomic, proteomic, and metabolomic)	Transcriptomic analysis revealed that TPP exposure markedly affected cell apoptosis, oncogene activation, REDOX homeostasis, DNA damage and repair. Additionally, proteomic analysis found that the related proteins associated with apoptosis, oxidative stress, metabolism and membrane structure were affected.	Ecotoxicol Environ Saf	2020 <sup>26</sup>
10	<i>In vitro</i>	MA-10 mouse Leydig tumor cells	superoxide production	All of the OPFRs significantly increased (10 $\mu$ M, 1.7-4.4-fold) superoxide production whereas BDE-47 had no significant effect. Basal progesterone production was significantly increased (10 $\mu$ M, 1.5 to 3-fold) by 2-ethylhexyl diphenyl phosphate, isodecyl diphenyl phosphate, isopropylated triphenyl phosphate, tert-butylphenyl diphenyl phosphate, and tricresyl phosphate, while BDE-47, triphenyl phosphate and tri-o-cresyl phosphate had no effect.	Toxicol Sci	2016 <sup>27</sup>
11	<i>In vitro</i>	HepG2 hepatoma cells, A549 lung cancer cells and Caco-2 colon	cell viability; reactive oxygen species (ROS) level	All these four OPFRs could inhibit cell viability, overproduce ROS level, induce DNA lesions and increase the LDH leakage.	J Environ Sci Health A Tox Hazard Subst Environ Eng	2016 <sup>28</sup>

		cancer cells						
12	<i>In vivo</i>	Male mice	Endocrine Oxidative stress	disruption;	Hepatic malondialdehyde (MDA) contents increased significantly in both TPP treated groups, while the contents of glutathione (GSH) decreased significantly in 300 mg/kg TPP and both TCEP treated groups. In addition, the hepatic activities of antioxidant enzymes including glutathione peroxidase (GPX), catalase (CAT) and glutathione S-transferase (GST) as well as their related gene expression were affected by TPP or TCEP exposure.	Environ Toxicol Pharmacol	2015 <sup>29</sup>	
13	<i>In vitro</i>	A549 cells	Intracellular ROS and miSOD analysis		The results of the intracellular ROS analysis showed that alkyl-PFRs could cause excessive production of ROS in the nucleus, indicating that PFRs can induce oxidative stress. TEHP and DNBP, which contain longer alkyl chains than the other alkyl-PFRs, induced severe oxidative damage.	Chemosphere	2020 <sup>30</sup>	
14	<i>Human</i>	Pregnant women	Oxidative stress biomarkers of MDA and 8-OHdG		Thyroid disrupting effects of OPE exposure on mothers and fetuses during pregnancy and the potential influence mediated by the oxidative stresses of DNA damage and lipid peroxidation.	Environ Int	2021 <sup>31</sup>	
Apoptosis	15	<i>In vitro</i>	JEG-3 cells	Lipid metabolism	Although PPAR $\gamma$ and its target CCAAT/enhancer binding proteins (C/EBP $\alpha$ ) was decreased, the TG content and gene expression of SREBP1, ACC, and CD36 decreased when TPP was co-exposed to the PPAR $\gamma$ antagonist GW9662. TPP also induced inflammatory responses, endoplasmic reticulum stress (ERS), and cell apoptosis.	Chemosphere	2021 <sup>32</sup>	
	16	<i>In vivo</i>	Weaned male mice (C57/BL6)	Metabolomic; transcriptomic	RNA-seq data indicated that neuronal transcription processes and cell apoptosis pathway (forkhead box (FOXO), and mitogen-activated protein kinase (MAPK) signaling pathways) were significantly affected by TPP exposure.	Chemosphere	2020 <sup>33</sup>	
	17	<i>In vitro</i>	Human normal liver cell (L02)	Transcriptomic; proteomic; metabolomic	TPP could induce human normal liver cell (L02) apoptosis, injury cell ultrastructure and elevate the levels of reactive oxygen species (ROS). Transcriptomic analysis revealed that TPP exposure markedly affected cell apoptosis, oncogene activation, REDOX homeostasis, DNA damage and repair. Additionally, proteomic analysis found that the related proteins associated with apoptosis, oxidative stress, metabolism and membrane structure were affected.	Ecotoxicol Environ Saf	2020 <sup>26</sup>	

	18	<i>In vivo</i>	Pregnant mice	the protein levels related to apoptosis	Western blot analysis verified that the protein levels related to ERS stress and apoptosis were significantly increased.	Environ Pollut	2022 <sup>34</sup>
	19	<i>In vitro</i>	Hepatocyte	mitochondrial injury; apoptosis inducing factor (AIF) release; reactive oxygen species (ROS) production; DNA damage; mitochondrial PARP1 dependent pathway	Docking view showed that TPP could interact with helix $\alpha$ J to affect the activation of PARP1 as a molecular initial event. In vitro assays suggested some biochemical events downstream of PARP1 activation, such as mitochondrial injury, apoptosis inducing factor (AIF) release, reactive oxygen species (ROS) production, and DNA damage. Moreover, the apoptosis was alleviated when cells were pretreated with PJ34 hydrochloride (PARP1 inhibitor), suggesting the mitochondrial PARP1 dependent pathway played a pivotal role in L02 cells apoptosis.	Ecotoxicol Environ Saf.	2021 <sup>35</sup>
Inflammasome	20	<i>In vitro</i>	Murine BV-2 microglia cells	NLRP3 inflammasome activation	TBBPA showed indications of possible secondary triggering activity while no changes were seen with TPP.	Chemosphere	2020 <sup>36</sup>
Glucocorticoid	21	<i>In vitro</i>	Hep G2 cell line	glucocorticoid, mineralocorticoid receptor antagonist activities	When HepG2 cells were exposed to TMPP, TPHP and TDBPP, the main metabolic sub-network disturbances focused on metabolism linked with oxidative stress, osmotic pressure equilibrium, and glucocorticoid and mineralocorticoid receptor antagonist activities.	Sci Total Environ	2019 <sup>16</sup>
	22	<i>In vitro</i>	CHO cells	CYP17,CYP21, CYP11B1 expression	TMPP, TPHP and TDBPP exhibited both GR and MR antagonistic activities.	Environ Sci Technol	2017 <sup>37</sup>
	23	<i>In vitro</i>	CHO-K1 cells and simian kidney COS-7 cells	glucocorticoid receptor (GR) antagonistic activities	Hydroxylated TPHP-metabolites also showed ER antagonistic activity at higher concentrations and exhibited pregnane X receptor (PXR) agonistic activity as well as androgen receptor (AR) and glucocorticoid receptor (GR) antagonistic activities at similar levels to those of TPHP.	Toxicol Lett	2016 <sup>38</sup>
	24	<i>In vitro</i>	CHO-K1 cell	glucocorticoid receptor (GR) antagonistic activity	TBP, tris(2-ethylhexyl) phosphate (TEHP), TDCPP, TPhP and TCP showed GR antagonistic activity.	Toxicology	2013 <sup>39</sup>

---

## Supplemental Figures

Figure S1. Pairwise spearman correlations of the 28 OPE exposures.

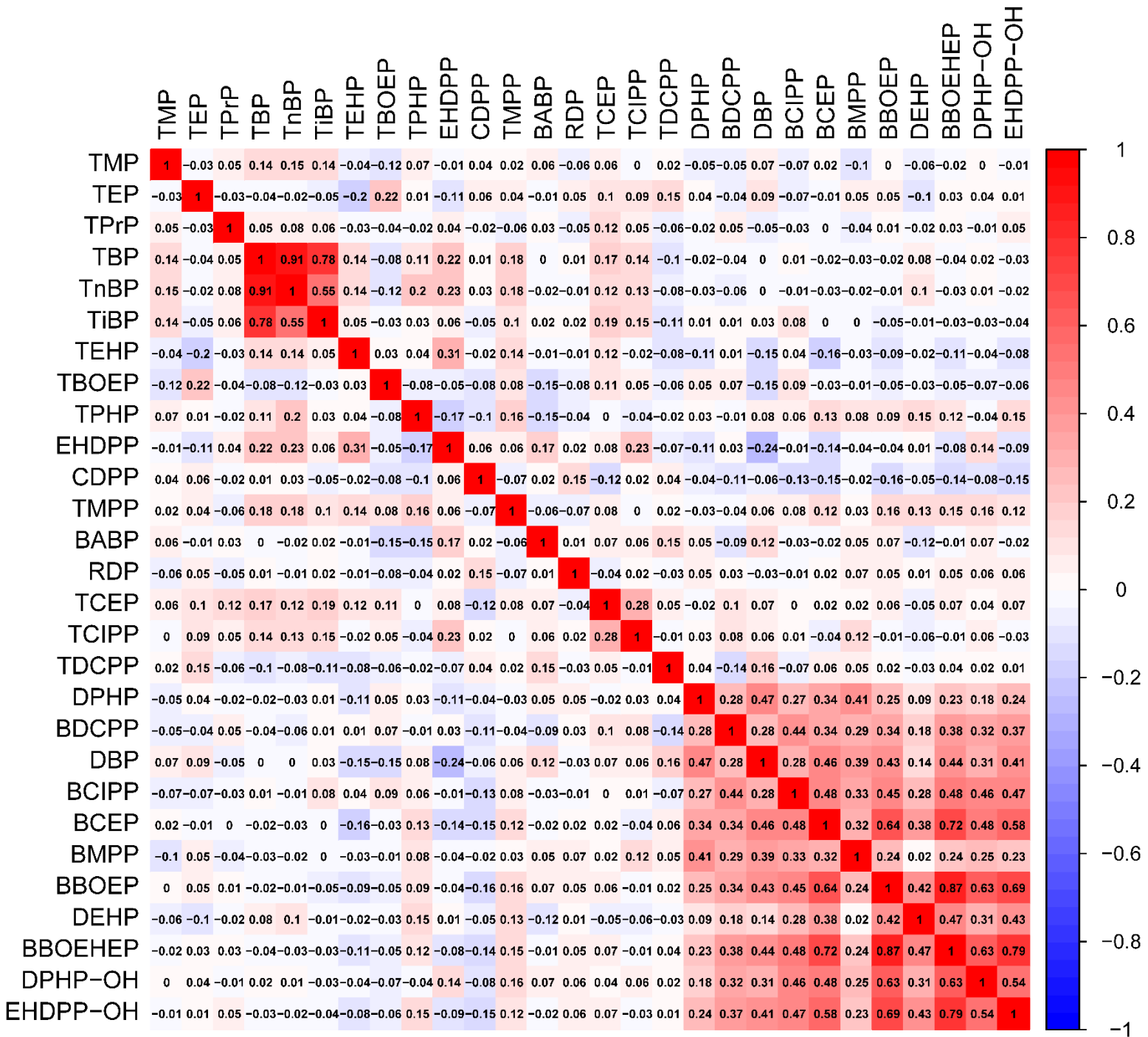




**Figure S2.** Sensitivity analysis results of the associations between OPE exposures and glycometabolic markers.

**(A)** Forest plot of the LMM results between OPE exposures and glycometabolic markers (FPG, GSP, FINS, and HOMA-IR) adjusting for age, sex, BMI, education level, financial income, blood cotinine concentration, other diets (3 days), and month of sample collection. **(B)** Forest plot of the LMM results between OPE exposures and glycometabolic markers (FPG, GSP, FINS, and HOMA-IR) adjusting for age, sex, BMI, education level, financial income, blood cotinine concentration, other diets (3 days), and cups of tea consumption (3 days). **(C)** Forest plot of the LMM results between OPEs exposures and glycometabolic markers (FPG, GSP, FINS, and HOMA-IR) adjusting for age, sex, BMI, education level, financial income, blood cotinine concentration, other diets (3 days), and frequency of alcohol consumption (3 days). The FDR adjusted *P*-values of each predictor are given as \* FDR < 0.05.

Note: see also **Excel Table S4**.

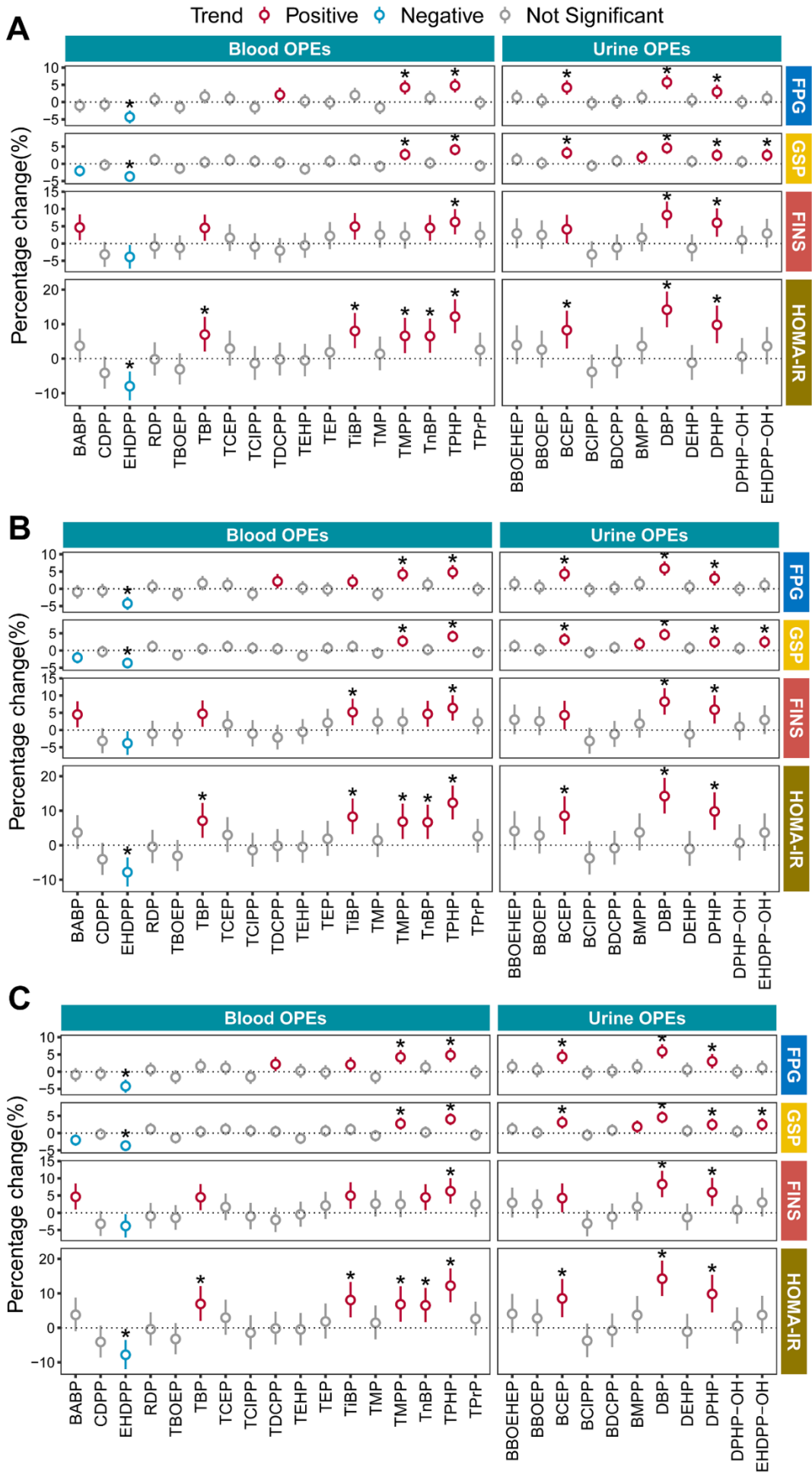


**Figure S3.** Stratification analysis results of the associations between OPE exposures and glycometabolic markers by sex.

Note: see also **Excel Table S5**.

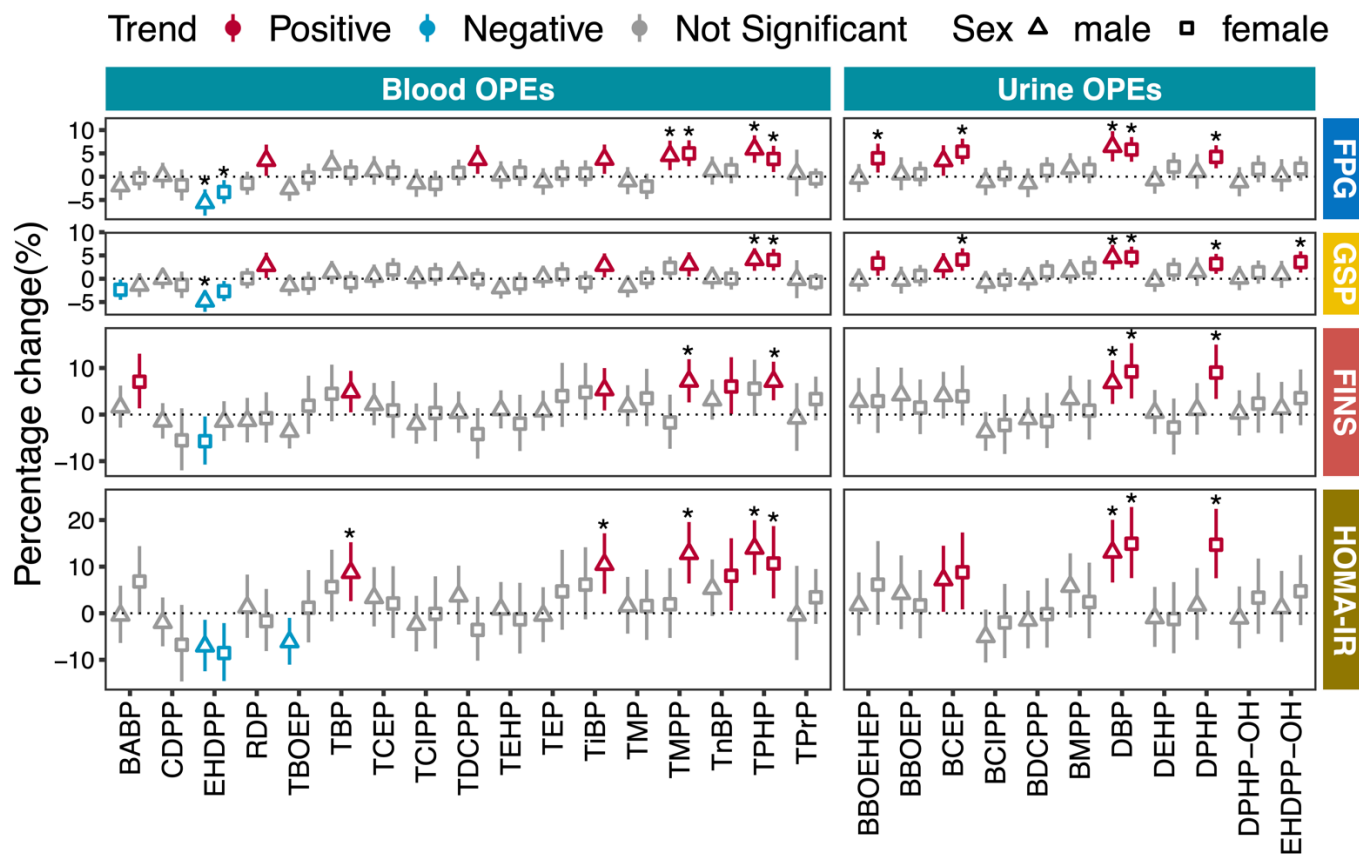
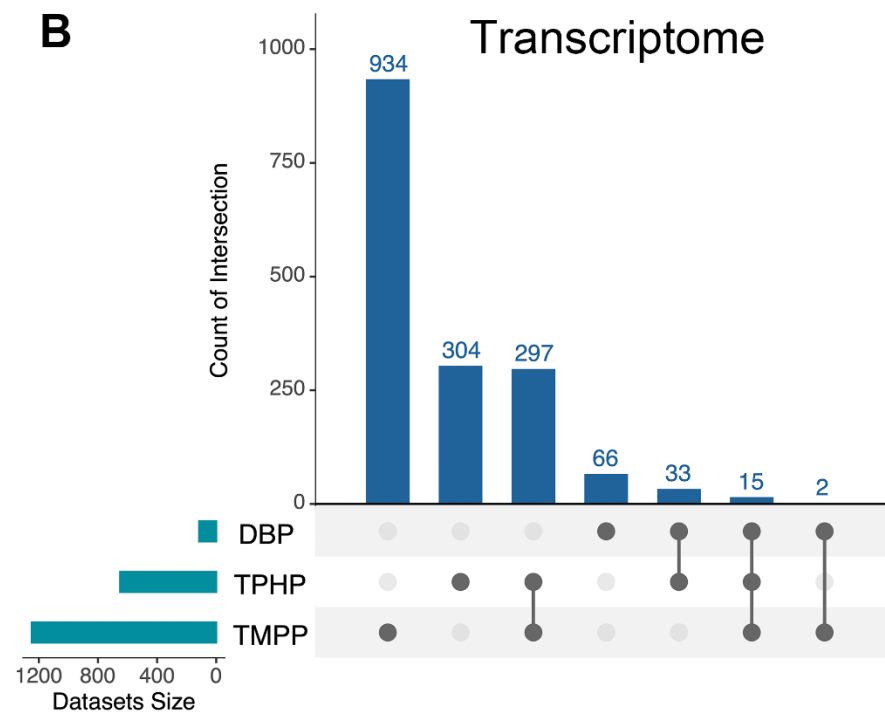
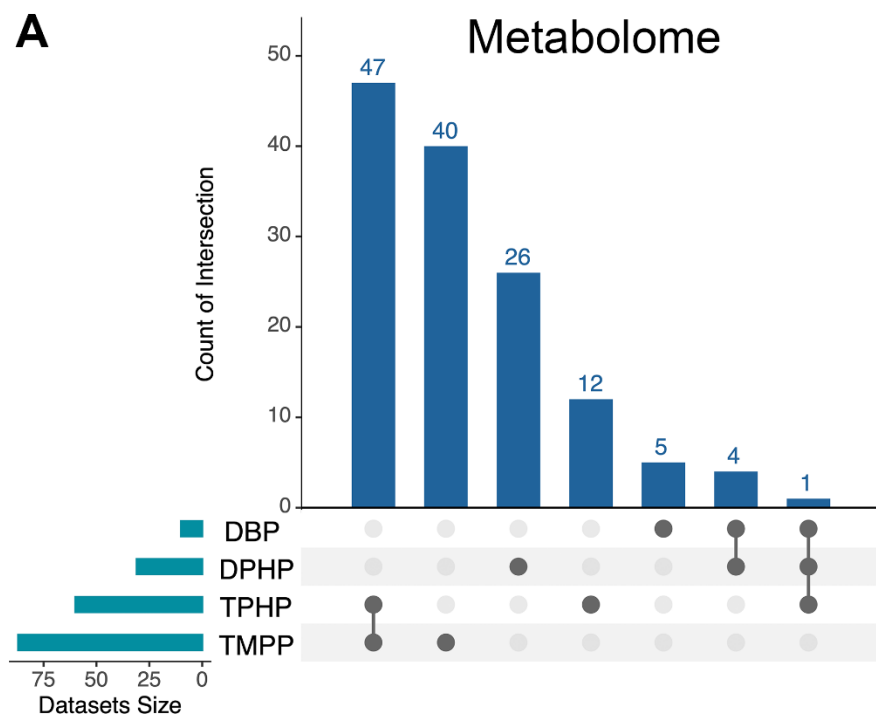


**Figure S4.** Common and specific biomolecular intermediators of individual OPEs.

(A) Upset plot of common and specific biomolecular intermediators of each OPE for metabolome. (B) Upset plot of common and specific biomolecular intermediators of each OPE for transcriptome.



## References

- 1 Wilmanski, T. *et al.* Blood metabolome predicts gut microbiome  $\alpha$ -diversity in humans. *Nature biotechnology* **37**, 1217-1228, doi:10.1038/s41587-019-0233-9 (2019).
- 2 Wang, C. *et al.* Triphenyl phosphate causes a sexually dimorphic metabolism dysfunction associated with disordered adiponectin receptors in pubertal mice. *Journal of hazardous materials* **388**, 121732, doi:10.1016/j.jhazmat.2019.121732 (2020).
- 3 Wang, D. *et al.* Effects of triphenyl phosphate exposure during fetal development on obesity and metabolic dysfunctions in adult mice: Impaired lipid metabolism and intestinal dysbiosis. *Environmental pollution (Barking, Essex : 1987)* **246**, 630-638, doi:10.1016/j.envpol.2018.12.053 (2019).
- 4 Wang, L., Huang, X., Laserna, A. K. C. & Li, S. F. Y. Untargeted metabolomics reveals transformation pathways and metabolic response of the earthworm *Perionyx excavatus* after exposure to triphenyl phosphate. *Scientific reports* **8**, 16440, doi:10.1038/s41598-018-34814-9 (2018).
- 5 Green, A. J. *et al.* Perinatal triphenyl phosphate exposure accelerates type 2 diabetes onset and increases adipose accumulation in UCD-type 2 diabetes mellitus rats. *Reproductive toxicology (Elmsford, N.Y.)* **68**, 119-129, doi:10.1016/j.reprotox.2016.07.009 (2017).
- 6 Du, Z. *et al.* TPhP exposure disturbs carbohydrate metabolism, lipid metabolism, and the DNA damage repair system in zebrafish liver. *Scientific reports* **6**, 21827, doi:10.1038/srep21827 (2016).
- 7 Philbrook, N. A., Restivo, V. E., Belanger, C. L. & Winn, L. M. Gestational triphenyl phosphate exposure in C57Bl/6 mice perturbs expression of insulin-like growth factor signaling genes in maternal and fetal liver. *Birth defects research* **110**, 483-494, doi:10.1002/bdr2.1185 (2018).
- 8 Wang, D. *et al.* Neonatal triphenyl phosphate and its metabolite diphenyl phosphate exposure induce sex- and dose-dependent metabolic disruptions in adult mice. *Environmental pollution (Barking, Essex : 1987)* **237**, 10-17, doi:10.1016/j.envpol.2018.01.047 (2018).
- 9 Adams, S. *et al.* Sex- and age-dependent effects of maternal organophosphate flame-retardant exposure on neonatal hypothalamic and hepatic gene expression. *Reproductive toxicology (Elmsford, N.Y.)* **94**, 65-74, doi:10.1016/j.reprotox.2020.04.001 (2020).
- 10 Walley, S. N. *et al.* Maternal organophosphate flame-retardant exposure alters offspring energy and glucose homeostasis in a sexually dimorphic manner in mice. *Journal of applied toxicology : JAT* **41**, 572-586, doi:10.1002/jat.4066 (2021).
- 11 Vail, G. M. *et al.* The interactions of diet-induced obesity and organophosphate flame retardant exposure on energy homeostasis in adult male and female mice. *Journal of toxicology and environmental health. Part A* **83**, 438-455, doi:10.1080/15287394.2020.1777235 (2020).
- 12 Krumm, E. A. *et al.* Organophosphate Flame-Retardants Alter Adult Mouse Homeostasis and Gene Expression in a Sex-Dependent Manner Potentially Through Interactions With ER $\alpha$ . *Toxicological sciences : an official journal of the Society of Toxicology* **162**, 212-224, doi:10.1093/toxsci/kfx238 (2018).
- 13 Vail, G. M. *et al.* Implications of peroxisome proliferator-activated receptor gamma (PPAR $\gamma$ ) with the intersection of organophosphate flame retardants and diet-induced obesity in adult mice. *Journal of toxicology and environmental health. Part A* **85**, 381-396, doi:10.1080/15287394.2021.2023716 (2022).
- 14 Vail, G. M. *et al.* Implications of estrogen receptor alpha (ER $\alpha$ ) with the intersection of organophosphate flame retardants and diet-induced obesity in adult mice. *Journal of toxicology and environmental health. Part A* **85**, 397-413, doi:10.1080/15287394.2022.2026849 (2022).
- 15 Liu, Y. *et al.* Remodeling on adipocytic physiology of organophosphorus esters in mature adipocytes. *Environmental pollution (Barking, Essex : 1987)* **305**, 119287, doi:10.1016/j.envpol.2022.119287 (2022).
- 16 Gu, J., Su, F., Hong, P., Zhang, Q. & Zhao, M. (1)H NMR-based metabolomic analysis of nine organophosphate flame retardants metabolic disturbance in Hep G2 cell line. *The Science of the total environment* **665**, 162-170, doi:10.1016/j.scitotenv.2019.02.055 (2019).
- 17 Cano-Sancho, G., Smith, A. & La Merrill, M. A. Triphenyl phosphate enhances adipogenic differentiation, glucose uptake

- and lipolysis via endocrine and noradrenergic mechanisms. *Toxicology in vitro : an international journal published in association with BIBRA* **40**, 280-288, doi:10.1016/j.tiv.2017.01.021 (2017).
- 18 Hu, W. *et al.* Triphenyl phosphate modulated saturation of phospholipids: Induction of endoplasmic reticulum stress and inflammation. *Environmental pollution (Barking, Essex : 1987)* **263**, 114474, doi:10.1016/j.envpol.2020.114474 (2020).
- 19 Umamaheswari, S., Karthika, P., Suvenitha, K., Kadirvelu, K. & Ramesh, M. Dose-Dependent Molecular Responses of Labeo rohita to Triphenyl Phosphate. *Chemical research in toxicology* **34**, 2500-2511, doi:10.1021/acs.chemrestox.1c00281 (2021).
- 20 Ramesh, M. *et al.* Organophosphorus flame retardant induced hepatotoxicity and brain AChE inhibition on zebrafish (Danio rerio). *Neurotoxicology and teratology* **82**, 106919, doi:10.1016/j.ntt.2020.106919 (2020).
- 21 Canbaz, D., Logiantara, A., van Ree, R. & van Rijt, L. S. Immunotoxicity of organophosphate flame retardants TPHP and TDCIPP on murine dendritic cells in vitro. *Chemosphere* **177**, 56-64, doi:10.1016/j.chemosphere.2017.02.149 (2017).
- 22 Van den Eede, N. *et al.* Metabolomics analysis of the toxicity pathways of triphenyl phosphate in HepaRG cells and comparison to oxidative stress mechanisms caused by acetaminophen. *Toxicology in vitro : an international journal published in association with BIBRA* **29**, 2045-2054, doi:10.1016/j.tiv.2015.08.012 (2015).
- 23 Yu, X. *et al.* OPFRs and BFRs induced A549 cell apoptosis by caspase-dependent mitochondrial pathway. *Chemosphere* **221**, 693-702, doi:10.1016/j.chemosphere.2019.01.074 (2019).
- 24 Mennillo, E., Cappelli, F. & Arukwe, A. Biotransformation and oxidative stress responses in rat hepatic cell-line (H4IIE) exposed to organophosphate esters (OPEs). *Toxicology and applied pharmacology* **371**, 84-94, doi:10.1016/j.taap.2019.04.004 (2019).
- 25 Chen, G. *et al.* TPP and TCEP induce oxidative stress and alter steroidogenesis in TM3 Leydig cells. *Reproductive toxicology (Elmsford, N.Y.)* **57**, 100-110, doi:10.1016/j.reprotox.2015.05.011 (2015).
- 26 Wang, X., Li, F., Liu, J., Ji, C. & Wu, H. Transcriptomic, proteomic and metabolomic profiling unravel the mechanisms of hepatotoxicity pathway induced by triphenyl phosphate (TPP). *Ecotoxicology and environmental safety* **205**, 111126, doi:10.1016/j.ecoenv.2020.111126 (2020).
- 27 Schang, G., Robaire, B. & Hales, B. F. Organophosphate Flame Retardants Act as Endocrine-Disrupting Chemicals in MA-10 Mouse Tumor Leydig Cells. *Toxicological sciences : an official journal of the Society of Toxicology* **150**, 499-509, doi:10.1093/toxsci/kfw012 (2016).
- 28 An, J. *et al.* The cytotoxicity of organophosphate flame retardants on HepG2, A549 and Caco-2 cells. *Journal of environmental science and health. Part A, Toxic/hazardous substances & environmental engineering* **51**, 980-9888, doi:10.1080/10934529.2016.1191819 (2016).
- 29 Chen, G., Jin, Y., Wu, Y., Liu, L. & Fu, Z. Exposure of male mice to two kinds of organophosphate flame retardants (OPFRs) induced oxidative stress and endocrine disruption. *Environmental toxicology and pharmacology* **40**, 310-318, doi:10.1016/j.etap.2015.06.021 (2015).
- 30 Yuan, S. *et al.* In vitro oxidative stress, mitochondrial impairment and G1 phase cell cycle arrest induced by alkyl-phosphorus-containing flame retardants. *Chemosphere* **248**, 126026, doi:10.1016/j.chemosphere.2020.126026 (2020).
- 31 Yao, Y. *et al.* Exposure to organophosphate ester flame retardants and plasticizers during pregnancy: Thyroid endocrine disruption and mediation role of oxidative stress. *Environment international* **146**, 106215, doi:10.1016/j.envint.2020.106215 (2021).
- 32 Wang, Y. *et al.* Triphenyl phosphate disturbs the lipidome and induces endoplasmic reticulum stress and apoptosis in JEG-3 cells. *Chemosphere* **275**, 129978, doi:10.1016/j.chemosphere.2021.129978 (2021).
- 33 Liu, X. *et al.* Triphenyl phosphate permeates the blood brain barrier and induces neurotoxicity in mouse brain. *Chemosphere* **252**, 126470, doi:10.1016/j.chemosphere.2020.126470 (2020).
- 34 Hong, J. *et al.* Prenatal exposure to triphenyl phosphate activated PPAR $\gamma$  in placental trophoblasts and impaired pregnancy outcomes. *Environmental pollution (Barking, Essex : 1987)* **301**, 119039, doi:10.1016/j.envpol.2022.119039 (2022).
- 35 Wang, X. *et al.* New insights into the mechanism of hepatocyte apoptosis induced by typical organophosphate ester: An integrated in vitro and in silico approach. *Ecotoxicology and environmental safety* **219**, 112342, doi:10.1016/j.ecoenv.2021.112342 (2021).

- 36 Bowen, C. *et al.* Mitochondrial-related effects of pentabromophenol, tetrabromobisphenol A, and triphenyl phosphate on murine BV-2 microglia cells. *Chemosphere* **255**, 126919, doi:10.1016/j.chemosphere.2020.126919 (2020).
- 37 Zhang, Q., Wang, J., Zhu, J., Liu, J. & Zhao, M. Potential Glucocorticoid and Mineralocorticoid Effects of Nine Organophosphate Flame Retardants. *Environmental science & technology* **51**, 5803-5810, doi:10.1021/acs.est.7b01237 (2017).
- 38 Kojima, H., Takeuchi, S., Van den Eede, N. & Covaci, A. Effects of primary metabolites of organophosphate flame retardants on transcriptional activity via human nuclear receptors. *Toxicology letters* **245**, 31-39, doi:10.1016/j.toxlet.2016.01.004 (2016).
- 39 Kojima, H. *et al.* In vitro endocrine disruption potential of organophosphate flame retardants via human nuclear receptors. *Toxicology* **314**, 76-83, doi:10.1016/j.tox.2013.09.004 (2013).